Fig. 5 Micro-CT analysis of humeri from wild-type (*Wt*), *lbab/lbab*, and *lbab/lbab*·CNP-Tg mice at the age of 10 weeks. *Scale bar* 1 mm

in *lbab/lbab* metatarsal explants than in *lbab/+* metatarsal explants and was returned to the same position as *lbab/+* metatarsal explants by addition of CNP (Fig. 8).

Discussion

Previously, we and other groups had reported in brief communications that the short stature phenotype of *lbab/lbab* mice is caused by a mutation in the CNP gene [11–13]. Here, we further analyzed the skeletal phenotypes of *lbab/lbab* mice and report the results in this full-length article.

Analysis of the growth curves of nasoanal and nose–tail lengths revealed that the shortness of *lbab/lbab* mice is mild at birth but rapidly progresses by the age of 3 weeks, and then, after 4 weeks, the ratio of the length of *lbab/lbab* mice compared to that of wild-type mice becomes almost constant. This suggests that CNP is especially crucial for the skeletal growth spurt that occurs in early life. Since CNP is expressed in the growth plate cartilage and works as an autocrine/paracrine regulator [5], CNP might affect the endochondral bone growth potently when the volume of growth plate cartilage is relatively abundant.

We confirmed the thinness of the growth plate of *lbab/lbab* mice, especially in its hypertrophic chondrocyte layer, followed by the impaired growth of long bones. The thinness of the growth plate of *lbab/lbab* mice was almost completely recovered by targeted overexpression of CNP in the growth plate by the age of 2 weeks. On the other hand, the recovery of the shortness of the total length of *lbab/lbab* bones by CNP was only partial at 2 weeks, becoming complete at the age of 10 weeks. This finding suggests that the recovery is evident earlier in the thickness of the growth plate than in the total bone length. In addition, immunohistochemistry for PCNA revealed that at the age of 2 weeks the proliferation of growth plate chondrocytes is decreased in *lbab/lbab* mice and that the decreased proliferation is not rescued by CNP overexpression, even though the thickness of the growth plate does fully recover.

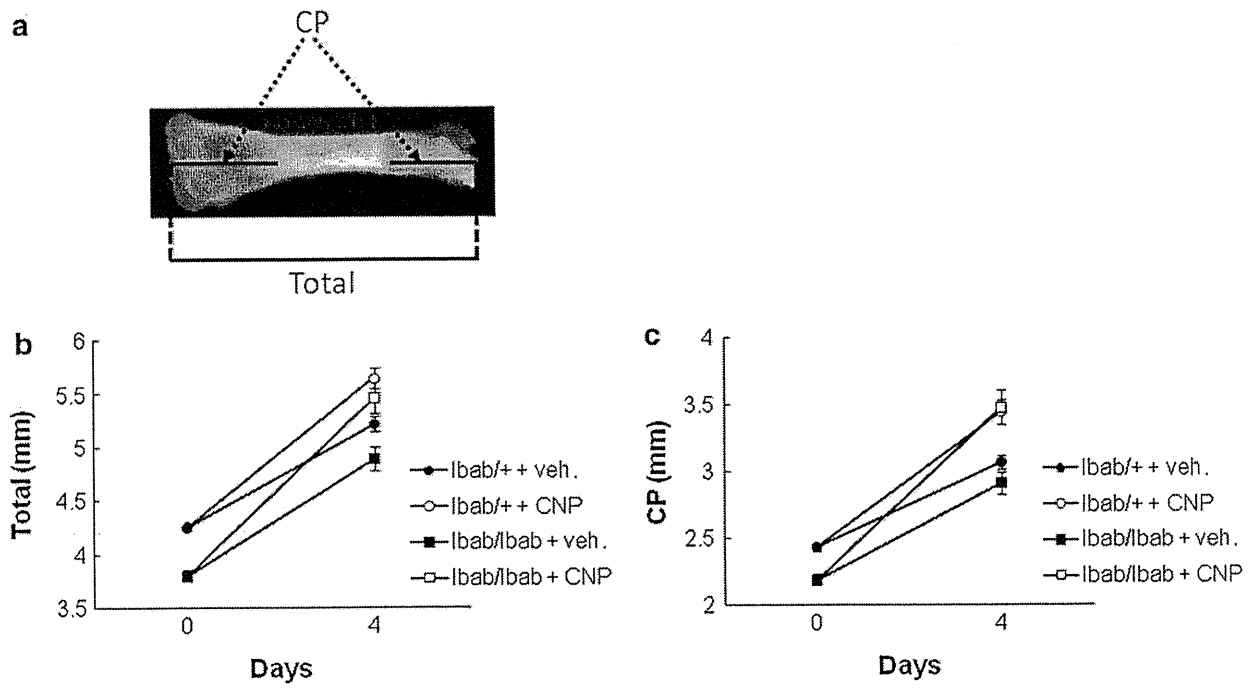

Fig. 6 Effect of CNP on cultured tibiae from fetal *lbab/+* and *lbab/lbab* mice. **a** A representative picture of a tibial explant from a fetal mouse. Total longitudinal length (*Total*) and the sum lengths of cartilaginous primordia (*CP*) are indicated. Graphs of total (**b**) and CP (**c**) lengths of cultured tibiae from *lbab/+* and *lbab/lbab* mice treated with vehicle (*veh.*) or 10^{-7} M CNP (*CNP*) for 4 days. *Circles* indicate *lbab/+* tibiae, and *squares* indicate *lbab/lbab* tibiae. At the end of culture, *closed symbols* indicate tibiae treated with vehicle and *open symbols* indicate those treated with CNP. n = 8–12 each

The reason the decreased proliferation of chondrocytes in the *lbab/lbab* growth plate was not rescued by CNP overexpression in chondrocytes is not clear, but it may be because of the weak and slow expression of the CNP transgene owing to the weak power of the promoter region. On the other hand, CNP could not increase the proliferation of growth plate chondrocytes in *lbab/lbab* explants in organ culture experiments in this study. The effect of CNP on chondrocyte proliferation might be so mild that other effects of CNP on growth plate chondrocytes, e.g., the stimulatory effect on matrix synthesis as we had previously reported [3, 4], might proceed to recover the thinned growth plate of *lbab/lbab* mice. The discrepancy between the effects on proliferation and matrix synthesis may explain in part the delayed recovery of bone length relative to growth plate thickness. On the other hand, immunohistochemical staining of type X collagen and Ihh in explanted growth plates at two different stages of endochondral ossification suggested that the progression of proliferative chondrocytes to hypertrophic chondrocytes was delayed in the *lbab/lbab* growth plate and recovered by addition of CNP. In addition to the result that the expression of MMP-13 was not different between the terminal hypertrophic chondrocytes of wild-type, *lbab/lbab*, and rescued growth plates, CNP might promote the hypertrophic differentiation of proliferative chondrocytes but not accelerate the terminal differentiation of hypertrophic chondrocytes.

In this study, we investigated the character of calcified bones of *lbab/lbab* mice using three-dimensional CT analysis: the bone volume of *lbab/lbab* mice was substantially decreased compared to that of wild-type mice and recovered by cartilage-specific CNP overexpression. The mechanism of decrease in bone volume of *lbab/lbab* mice is still unknown, but CNP may be expressed in and affect cells other than chondrocytes, i.e., osteoblasts or osteoclasts, in bone. Although overexpression of CNP was targeted to chondrocytes in our rescue experiments, early onset of CNP-Tg expression from the CP might have been able to affect bone metabolism at the earlier stage of skeletogenesis [17] and may have continued to affect osteoblasts or osteoclasts near the growth plate cartilage in the later stage of skeletogenesis. Whereas several in vitro effects of CNP on osteoblastic cell lineages or osteoclasts have been reported [18–28], the in vivo effects of CNP on bone metabolism remain elusive; and further experiments are now ongoing in our laboratory.

We previously discovered that in two strains of mice, *cn/cn* and *slw/slw*, dwarfism is caused by spontaneous

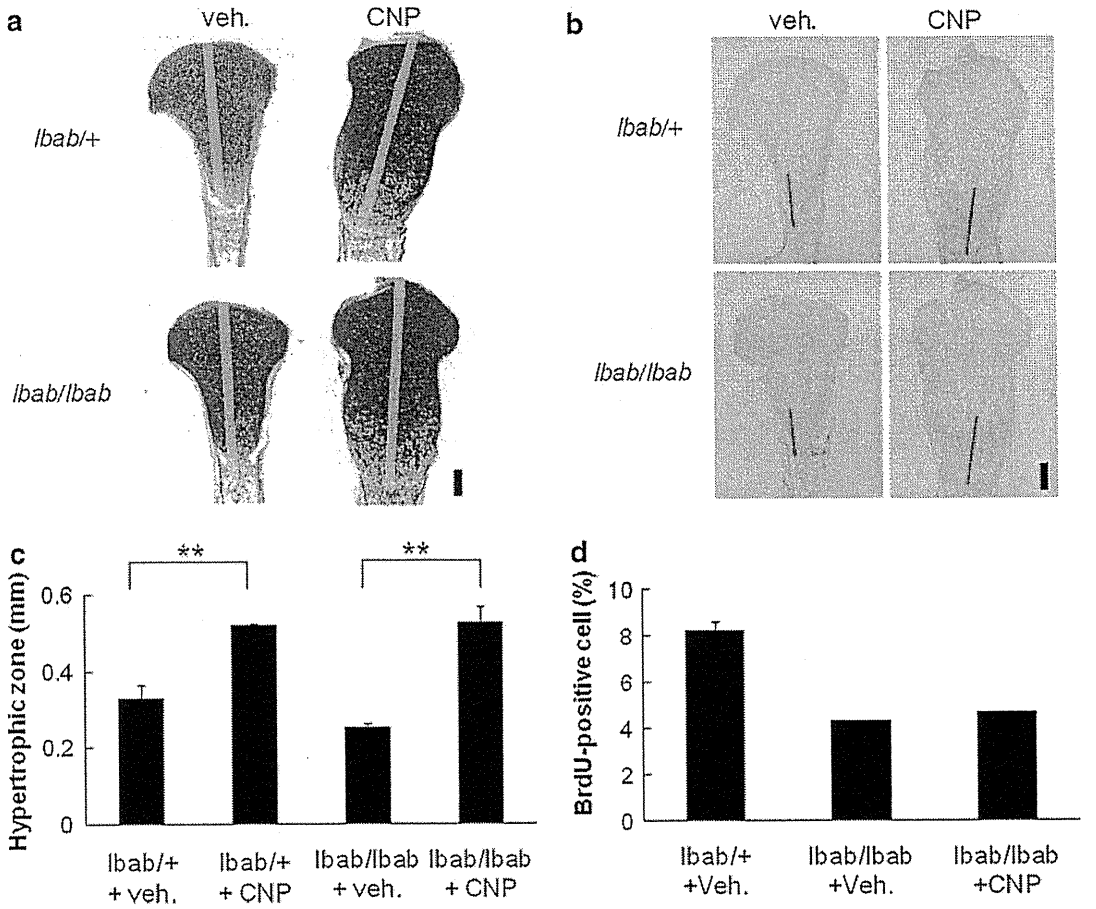

Fig. 7 Histological analyses of the growth plates of tibial explants from fetal *lbab/+* and *lbab/lbab* mice treated with vehicle (*veh.*) or 10^{-7} M CNP (*CNP*) for 4 days. Alcian blue and hematoxylin–eosin staining (**a**) and immunohistochemical staining for type X collagen (**b**). *Yellow bars* in **a** indicate lengths of cartilaginous primordial, and *red bars* in **b** indicate heights of hypertrophic chondrocyte layers. *Scale bars* 200 μm. Height of hypertrophic chondrocyte layer (**c**) and proportion of BrdU-positive cells (**d**) of the growth plate of tibial explant from fetal *lbab/+* or *lbab/lbab* mice treated with 10^{-7} M CNP or vehicle at the end of the 4-day culture period. $n = 3$ each. $^{**}P < 0.01$ in **c** and $n = 2$–3 each in **d** (Color figure online)

mutations in the GC-B gene [7, 8]. In humans, it has been identified that AMDM is caused by spontaneous loss-of-function mutations in the GC-B gene [9, 29]. The *lbab/lbab* mouse, the skeletal phenotype of which we have closely analyzed in the present report, has a spontaneous loss-of-function mutation in the CNP gene; by analogy to the GC-B gene, some forms of human skeletal dysplasia might be caused by mutations in the CNP gene. Thus far, no such conditions have been discovered [30]. In the event such a discovery is made, the *lbab/lbab* mouse would then be a novel model of a form of human skeletal dysplasia caused by a mutation in the CNP gene.

In contrast to mice homozygous for the *lbab* allele, the growth and skeletal phenotype of mice heterozygous for the *lbab* allele were not different from those of wild-type mice, as is the case with heterozygous CNP knockout mice. This confirms that haploinsufficiency for the CNP gene does not exist in mice. Likewise, heterozygotes for the GC-B knockout, the *cn* allele, or the *slw* allele exhibit no skeletal abnormalities [6–8]; thus, haploinsufficiency of the GC-B gene also does not exist in mice. Nevertheless, haploinsufficiency of the GC-B gene does exist in humans: heterozygous carriers of AMDM are reported to be shorter than expected for their population of origin [31]. The reason for the discrepancy is not clear at present, but it may have to do with differences between species or some other unknown mechanism(s). We will have to perform further investigations on the skeletal phenotypes of the aforementioned lines of GC-B mutant mice; such experiments are now ongoing in our laboratory.

In summary, in this study we more closely investigated the skeletal phenotypes of a novel CNP mutant mouse, *lbab/lbab*. The results of this study will be useful not only for further elucidation of the physiological role of CNP on

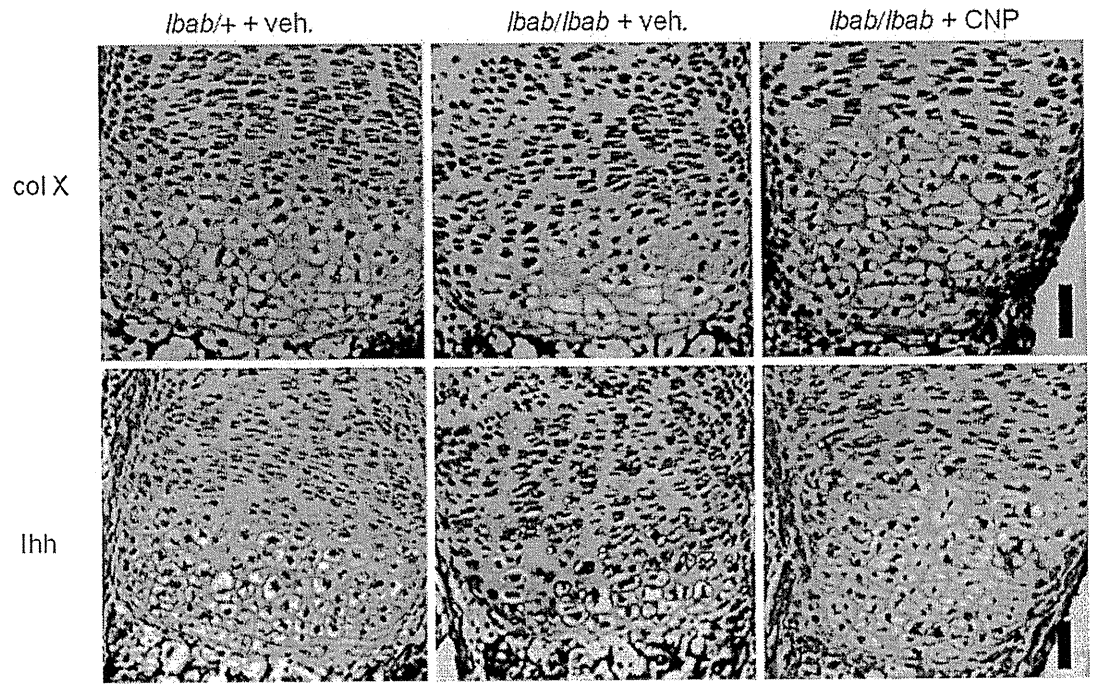

Fig. 8 Immunohistochemical staining of type X collagen (*upper panels*) and Ihh (*lower panels*) of the growth plates of metatarsal explants from fetal *lbab/+* and *lbab/lbab* mice treated with vehicle (*veh.*) or 10^{-7} M CNP for 4 days. *Scale bar* 50 μm

endochondral bone growth but also for the prediction of pathophysiology of a hypothetical chondrodysplasia caused by a mutation in the human CNP gene, which has not yet been discovered.

Acknowledgments We thank B. de Crombrugghe (Department of Genetics, University of Texas M.D. Anderson Cancer Center) for the *Col2a1* promoter. This study was supported by a Grant-in-Aid for Scientific Research from the Ministry of Health, Labor, and Welfare of Japan and the Ministry of Education, Culture, Sports, Sciences, and Technology of Japan (21591176, 21119013).

References

1. Nakao K, Ogawa Y, Suga S, Imura H (1992) Molecular biology and biochemistry of the natriuretic peptide system. I: Natriuretic peptides. J Hypertens 10:907–912
2. Nakao K, Ogawa Y, Suga S, Imura H (1992) Molecular biology and biochemistry of the natriuretic peptide system. II: Natriuretic peptide receptors. J Hypertens 10:1111–1114
3. Yasoda A, Komatsu Y, Chusho H, Miyazawa T, Ozasa A, Miura M, Kurihara T, Rogi T, Tanaka S, Suda M, Tamura N, Ogawa Y, Nakao K (2004) Overexpression of CNP in chondrocytes rescues achondroplasia through a MAPK-dependent pathway. Nat Med 10:80–86
4. Kake T, Kitamura H, Adachi Y, Yoshioka T, Watanabe T, Matsushita H, Fujii T, Kondo E, Tachibe T, Kawase Y, Jishage K, Yasoda A, Mukoyama M, Nakao K (2009) Chronically elevated plasma C-type natriuretic peptide level stimulates skeletal growth in transgenic mice. Am J Physiol Endocrinol Metab 297:E1339–E1348
5. Chusho H, Tamura N, Ogawa Y, Yasoda A, Suda M, Miyazawa T, Nakamura K, Nakao K, Kurihara T, Komatsu Y, Itoh H, Tanaka K, Saito Y, Katsuki M, Nakao K (2001) Dwarfism and early death in mice lacking C-type natriuretic peptide. Proc Natl Acad Sci USA 98:4016–4021
6. Tamura N, Doolittle LK, Hammer RE, Shelton JM, Richardson JA, Garbers DL (2004) Critical roles of the guanylyl cyclase B receptor in endochondral ossification and development of female reproductive organs. Proc Natl Acad Sci USA 101:17300–17305
7. Tsuji T, Kunieda T (2005) A loss-of-function mutation in natriuretic peptide receptor 2 (*Npr2*) gene is responsible for disproportionate dwarfism in *cn/cn* mouse. J Biol Chem 280: 14288–14292
8. Sogawa C, Tsuji T, Shinkai Y, Katayama K, Kunieda T (2007) Short-limbed dwarfism: *slw* is a new allele of Npr2 causing chondrodysplasia. J Hered 98:575–580
9. Bartels CF, Bükülmez H, Padayatti P, Rhee DK, van Ravenswaaij-Arts C, Pauli RM, Mundlos S, Chitayat D, Shih LY, Al-Gazali LI, Kant S, Cole T, Morton J, Cormier-Daire V, Faivre L, Lees M, Kirk J, Mortier GR, Leroy J, Zabel B, Kim CA, Crow Y, Braverman NE, van den Akker F, Warman ML (2004) Mutations in the transmembrane natriuretic peptide receptor NPR-B impair skeletal growth and cause acromesomelic dysplasia, type Maroteaux. Am J Hum Genet 75:27–34
10. The Jackson Laboratory. http://www.jax.org/index.html
11. Jiao Y, Yan J, Jiao F, Yang H, Donahue LR, Li X, Roe BA, Stuart J, Gu W (2007) A single nucleotide mutation in Nppc is associated with a long bone abnormality in *lbab* mice. BMC Genet 8:16
12. Tsuji T, Kondo E, Yasoda A, Inamoto M, Kiyosu C, Nakao K, Kunieda T (2008) Hypomorphic mutation in mouse *Nppc* gene

causes retarded bone growth due to impaired endochondral ossification. Biochem Biophys Res Commun 376:186–190
13. Yoder AR, Kruse AC, Earhart CA, Ohlendorf DH, Potter LR (2008) Reduced ability of C-type natriuretic peptide (CNP) to activate natriuretic peptide receptor B (NPR-B) causes dwarfism in *lbab-/-* mice. Peptides 29:1575–1581
14. Suda M, Ogawa Y, Tanaka K, Tamura N, Yasoda A, Takigawa T, Uehira M, Nishimoto H, Itoh H, Saito Y, Shiota K, Nakao K (1998) Skeletal overgrowth in transgenic mice that overexpress brain natriuretic peptide. Proc Natl Acad Sci USA 95:2337–2342
15. Yasoda A, Ogawa Y, Suda M, Tamura N, Mori K, Sakuma Y, Chusho H, Shiota K, Tanaka K, Nakao K (1998) Natriuretic peptide regulation of endochondral ossification. Evidence for possible roles of the C-type natriuretic peptide/guanylyl cyclase-B pathway. J Biol Chem 273:11695–11700
16. Vortkamp A, Lee K, Lanske B, Segre GV, Kronenberg HM, Tabin CJ (1996) Regulation of rate of cartilage differentiation by Indian hedgehog and PTH-related protein. Science 273:613–622
17. Zhou G, Garofalo S, Mukhopadhyay K, Lefebvre V, Smith CN, Eberspaecher H, de Crombrugghe B (1995) A 182 bp fragment of the mouse pro alpha 1(II) collagen gene is sufficient to direct chondrocyte expression in transgenic mice. J Cell Sci 108(Pt 12): 3677–3684
18. Inoue A, Hiruma Y, Hirose S, Yamaguchi A, Furuya M, Tanaka S, Hagiwara H (1996) Stimulation by C-type natriuretic peptide of the differentiation of clonal osteoblastic MC3T3-E1 cells. Biochem Biophys Res Commun 221:703–707
19. Hagiwara H, Inoue A, Yamaguchi A, Yokose S, Furuya M, Tanaka S, Hirose S (1996) cGMP produced in response to ANP and CNP regulates proliferation and differentiation of osteoblastic cells. Am J Physiol Cell Physiol 270:C1311–C1318
20. Suda M, Tanaka K, Fukushima M, Natsui K, Yasoda A, Komatsu Y, Ogawa Y, Itoh H, Nakao K (1996) C-type natriuretic peptide as an autocrine/paracrine regulator of osteoblast. Evidence for possible presence of bone natriuretic peptide system. Biochem Biophys Res Commun 223:1–6
21. Yanaka N, Akatsuka H, Kawai E, Omori K (1998) 1,25-Dihydroxyvitamin D_3 upregulates natriuretic peptide receptor-C expression in mouse osteoblasts. Am J Physiol Endocrinol Metab 275:E965–E973
22. Inoue A, Hayakawa T, Otsuka E, Kamiya A, Suzuki Y, Hirose S, Hagiwara H (1999) Correlation between induction of expression of biglycan and mineralization by C-type natriuretic peptide in osteoblastic cells. J Biochem 125:103–108
23. Suda M, Komatsu Y, Tanaka K, Yasoda A, Sakuma Y, Tamura N, Ogawa Y, Nakao K (1999) C-type natriuretic peptide/guanylate cyclase B system in rat osteogenic ROB-C26 cells and its down-regulation by dexamethazone. Calcif Tissue Int 65:472–478
24. Inoue A, Kamiya A, Ishiji A, Hiruma Y, Hirose S, Hagiwara H (2000) Vasoactive peptide-regulated gene expression during osteoblastic differentiation. J Cardiovasc Pharmacol 36:S286–S289
25. Inoue A, Kobayashi Y, Ishizuka M, Hirose S, Hagiwara H (2002) Identification of a novel osteoblastic gene, inducible by C-type natriuretic peptide, whose transcript might function in mineralization as a noncoding RNA. Calcif Tissue Int 70:111–116
26. Yeh LC, Zavala MC, Lee JC (2006) C-type natriuretic peptide enhances osteogenic protein-1-induced osteoblastic cell differentiation via Smad5 phosphorylation. J Cell Biochem 97:494–500
27. Kaneki H, Kurokawa M, Ide H (2008) The receptor attributable to C-type natriuretic peptide-induced differentiation of osteoblasts is switched from type B- to type C-natriuretic peptide receptor with aging. J Cell Biochem 103:753–764
28. Holliday LS, Dean AD, Greenwald JE, Glucks SL (1995) C-type natriuretic peptide increases bone resorption in 1,25-dihydroxyvitamin D_3–stimulated mouse bone marrow cultures. J Biol Chem 270:18983–18989
29. Hachiya R, Ohashi Y, Kamei Y, Suganami T, Mochizuki H, Mitsui N, Saitoh M, Sakuragi M, Nishimura G, Ohashi H, Hasegawa T, Ogawa Y (2007) Intact kinase homology domain of natriuretic peptide receptor-B is essential for skeletal development. J Clin Endocrinol Metab 92:4009–4014
30. Superti-Furga A, Unger S (2007) Nosology and classification of genetic skeletal disorders: 2006 revision. Am J Med Genet A 143:1–18
31. Olney RC, Bükülmez H, Bartels CF, Prickett TC, Espiner EA, Potter LR, Warman ML (2006) Heterozygous mutations in natriuretic peptide receptor-B (NPR2) are associated with short stature. J Clin Endocrinol Metab 91:1229–1232

Forkhead Box A1 (FOXA1) and A2 (FOXA2) Oppositely Regulate Human Type 1 Iodothyronine Deiodinase Gene in Liver

Naotetsu Kanamoto, Tetsuya Tagami, Yoriko Ueda-Sakane, Masakatsu Sone, Masako Miura, Akihiro Yasoda, Naohisa Tamura, Hiroshi Arai, and Kazuwa Nakao

Department of Medicine and Clinical Science, Kyoto University Graduate School of Medicine (N.K., Y.U.-S., M.S., M.M., A.Y., N.T., H.A., K.N.), Kyoto 606-8507, Japan; and Division of Endocrinology and Metabolism, Clinical Research Institute, National Hospital Organization Kyoto Medical Center (T.T.), Kyoto 612-8555, Japan

Type 1 iodothyronine deiodinase (D1), a selenoenzyme that catalyzes the bioactivation of thyroid hormone, is expressed mainly in the liver. Its expression and activity are modulated by several factors, but the precise mechanism of its transcriptional regulation remains unclear. In the present study, we have analyzed the promoter of human D1 gene (*hDIO1*) to identify factors that prevalently increase D1 activity in the human liver. Deletion and mutation analyses demonstrated that a forkhead box (FOX)A binding site and an E-box site within the region between nucleotides −187 and −132 are important for *hDIO1* promoter activity in the liver. EMSA demonstrated that FOXA1 and FOXA2 specifically bind to the FOXA binding site and that upstream stimulatory factor (USF) specifically binds to the E-box element. Overexpression of FOXA2 decreased *hDIO1* promoter activity, and short interfering RNA-mediated knockdown of FOXA2 increased the expression of *hDIO1* mRNA. In contrast, overexpression of USF1/2 increased *hDIO1* promoter activity. Short interfering RNA-mediated knockdown of FOXA1 decreased the expression of *hDIO1* mRNA, but knockdown of both FOXA1 and FOXA2 restored it. The response of the *hDIO1* promoter to USF was greatly attenuated in the absence of FOXA1. Taken together, these results indicate that a balance of FOXA1 and FOXA2 expression modulates *hDIO1* expression in the liver. **(*Endocrinology* 153: 492–500, 2012)**

Thyroid hormone activation and inactivation are mediated by three selenoenzymes, type 1 iodothyronine deiodinase (D1), D2, and D3. D1 and D2 catalyze the conversion of T_4 to T_3 via removal of outerring iodine (1). The human D1 gene (*hDIO1*) is expressed in the liver, kidney, thyroid, and pituitary (2). The D2 gene is expressed in the central nervous system, pituitary, heart, and skeletal muscle, but it is absent in the liver (1). The D3 gene is expressed in the central nervous system and placenta, and it is involved in thyroid hormone inactivation by mediating the removal of innerring iodine. Unlike D2, D1 activity is considered to be regulated predominantly at the pretranslational level. The expression and activity of D1 are modulated by a variety of factors. T_3 induces the expression of *hDIO1* via two thyroid hormone responsive elements within its promoter (3), and nuclear factor κB induced by TNFα inhibits the T_3-dependent induction of D1 (4). However, the precise mechanism of the transcriptional regulation of *hDIO1* expression remains unclear.

In this study, we sought to identify factors that increased D1 activity in the liver, a main organ that expresses *hDIO1*. We assessed the promoter activity of the 5-kb 5′-flanking region of *hDIO1* and characterized regulatory element-binding proteins within this region. In this study, we identify responsive elements for the forkhead box (FOX) transcription factors FOXA1/FOXA2 and the ba-

ISSN Print 0013-7227 ISSN Online 1945-7170
Printed in U.S.A.

doi: 10.1210/en.2011-1310 Received May 30, 2011. Accepted October 17, 2011.
First Published Online November 8, 2011

Abbreviations: D1, Type 1 iodothyronine deiodinase; FOX, forkhead box; *hDIO1*, human D1 gene; HNF, hepatocyte nuclear factor; MUT, mutated oligonucleotide; siRNA, short interfering RNA; USF, upstream stimulatory factor; WT, wild type.

sic/helix-loop-helix-leucine zipper transcription factor upstream stimulatory factor (USF), and we show that FOXA1, FOXA2, and USF all participate in the regulation of *hDIO1*. We also show that FOXA1 is required for the activation of the *hDIO1* promoter by USF and that FOXA2 represses the transcription of *hDIO1* and disrupts the interaction of USF with FOXA1 by occupying the FOXA binding site. Collectively, these results demonstrate that FOXA1 and FOXA2 display opposing activity in the regulation of *hDIO1* expression in the liver.

Materials and Methods

Cell culture

The human liver carcinoma cell line HepG2 was obtained from American Type Culture Collection (Manassas, VA) and cultured in MEM (Life Technologies, Carlsbad, CA) with 0.1 mM nonessential amino acid solution (Life Technologies), 1 mM sodium pyruvate (Life Technologies), 100 U/ml penicillin, 100 μg/ml streptomycin, and 0.25 μg/ml amphotericin B supplemented with 10% fetal bovine serum (Sigma-Aldrich, St. Louis, MO) at 37 C in a humidified atmosphere containing 5% CO_2. TSA 201 cells, a clone of human embryonic kidney 293 cells (5), were cultured in DMEM (Life Technologies) with 100 U/ml penicillin, 100 μg/ml streptomycin, and 0.25 μg/ml amphotericin B supplemented with 10% fetal bovine serum at 37 C in a humidified atmosphere containing 5% CO_2.

Plasmid construction

Deletion mutants of the 5′-flanking regions of *hDIO1* (−4949, −2023, −343, −187, −150, −131, and −103/−4, the translational start site was set at +1) were prepared by PCR using human genomic DNA from leukocytes as a template. The resulting PCR products were subcloned into *Eco*RV or *Kpn*I/*Hin*dIII-digested pGL4.10 (Promega, Madison, WI) to create a fusion with the luciferase gene (−4949, −2023, −343, −187, −150, −131, and −103/−4 hDIO1-Luc). The PCR primers, containing *Eco*RV, *Kpn*I, or *Hin*dIII linker, are listed in Table 1. The correct orientation of these deletion mutant constructs was confirmed by sequencing.

Mutations were created using the QuikChange Site-Directed Mutagenesis kit (Stratagene, La Jolla, CA), according to the manufacturer's instruction; −187/−4 and −150/−4 hDIO1-Luc were used as templates. For mutagenesis, the sequences of the FOXA binding element and E-box were specified in figure 3 below. Mutated constructs were isolated from each reaction and verified by sequencing.

Plasmids expressing cDNA for FOXA2 and USF1, pF1KB7038 and pF1KB8339, respectively, were generated by Kazusa DNA Research Institute (Chiba, Japan) and purchased from Promega. These plasmids were digested with *Sgf*I and *Pme*I, and cDNA for FOXA2 and USF1 were ligated into the *Sgf*I/*Pme*I-digested pF4A CMV Flexi vector (Promega), which uses the human cytomegalovirus intermediate-early enhancer/promoter to allow constitutive protein expression at native levels in mammalian cells. The open reading frame of human USF2 was generated by PCR using HeLa cell cDNA as a template. The PCR primers containing *Sgf*I or *Pme*I linker are listed in Table 1. The PCR product was digested with *Sgf*I and *Pme*I, cloned into the *Sgf*I/*Pme*I-digested pF4A CMV Flexi vector, and verified by sequencing.

Transient transfection and luciferase assay

HepG2 and TSA 201 cells were plated at 1.5–2 × 10^5 and 0.5–1 × 10^5 cells/well in 24-well tissue culture plates, respectively. Cells were maintained in 0.5 ml of antibiotic-free medium for 1 d before transfection. Transient transfections were performed using the Lipofectamine LTX reagent (Life Technologies) for HepG2 cells and the Lipofectamine 2000 reagent (Life Technologies) for TSA 201 cells according to the manufacturer's instruction. In HepG2 cells, transfections included 500 ng of experimental reporter constructs and 25 ng of pGL4.74, which contained the cDNA encoding *Renilla* luciferase (Promega) as an internal control for transfection efficiency. In TSA 201 cells, transfections included 100 ng of experimental reporter constructs and 5 ng of pGL4.74. In the experiments with plasmids expressing FOXA2 and/or USF, total amount of plasmid DNA was kept constant by adding the corresponding amount of pF4A without a cDNA insert. After transfection, cells were grown in antibiotic-free medium and harvested after 48 h. Luciferase activity was determined using the Dual-Luciferase Reporter Assay System (Promega), and luminescence was measured by a 2030 ARVOX multilabel reader (PerkinElmer, Waltham, MA). Firefly luciferase activity was normalized to *Renilla* luciferase activity in each well to control for transfection efficiency.

Computational analysis of the putative transcription factor binding sites

The putative transcription factor binding sites on the 5′-flanking region of *hDIO1* were identified by computational

TABLE 1. Oligonucleotides used in plasmid construction and RT-PCR

	Forward primer (5′-3′)	Reverse primer (5′-3′)	Accession no.
Plusmid construction			
−4949/−4 hdio1-Luc	GGGGATATCGCAGGTGCAGCCTAGAGATGTAACG	CCCAAGCTTGGCAAAGCCAGAGTAAGCTC	AL031427
−2023/−4 hdio1-Luc	CGGGGTACCACACTTCCATTCCAGTTACAG	CCCAAGCTTGGCAAAGCCAGAGTAAGCTC	AL031427
−343/−4 hdio1-Luc	CGGGGTACCGAGAGAGCATCTAACAGGTTC	CCCAAGCTTGGCAAAGCCAGAGTAAGCTC	AL031427
−187/−4 hdio1-Luc	CGGGGTACCGACCTTTGTGCACCTGGTTAG	CCCAAGCTTGGCAAAGCCAGAGTAAGCTC	AL031427
−150/−4 hdio1-Luc	CGGGGTACCGACAGAAAGGCAAACATCTTC	CCCAAGCTTGGCAAAGCCAGAGTAAGCTC	AL031427
−131/−4 hdio1-Luc	CGGGGTACCTCTGACCTGACTCCTTCCCCTG	CCCAAGCTTGGCAAAGCCAGAGTAAGCTC	AL031427
−103/−4 hdio1-Luc	CGGGGTACCGGTTGGCTGCTCCTACCCTGC	CCCAAGCTTGGCAAAGCCAGAGTAAGCTC	AL031427
pF4A-USF2	AGCAGCGATCGCCATGGACATGCTGGACCCGGGTCTGGA	CGAGGTTTAAACCTGCCGGGTGCCCTCGCCCA	NM_003367
RT-PCR			
hDIO1	CAGAGTCAAGCGGAACATCC	CCGTTGGTCACCTAGAATTG	NM_000792
Cyclophilin A	GCACTGGAGAGAAAGGATTTGG	CAGCAATGGTGATCTTCTTGC	NM_021130

analysis using TFSEARCH databases (http://www.cbrc.jp/research/db/TFSEARCHJ.html), based on the TRANSFAC databases (6).

RNA isolation, RT-PCR, and quantitative PCR

Total RNA was extracted from HepG2 cells using the RNeasy Plus Mini kit (QIAGEN, Valencia, CA) according to the manufacturer's instruction. One microgram of total RNA was reverse transcribed with random hexamers using a First-strand cDNA Synthesis kit (GE Healthcare UK Ltd., Buckinghamshire, UK) according to the manufacturer's instruction. The resulting cDNA were diluted 1:10 and subjected to PCR amplification with 0.5 mM each of the sense and antisense primers and 0.5 U of AmpliTaq Gold DNA polymerase (Life Technologies). The PCR primers used for *hDIO1* and human cyclophilin A gene are indicated in Table 1. The PCR conditions were 40 cycles of denaturation for 1 min at 95 C, annealing for 1 min at 52 C, and extension for 1 min at 72 C. The PCR products were electrophoresed in 2% agarose gels.

Quantitative PCR reactions were performed, recorded, and analyzed using TaqMan Gene Expression Assays with StepOnePlus real-time PCR system (Life Technologies). The probe and primers were Hs00270129_m1 (human *FOXA1*), Hs00232764_m1 (human *FOXA2*), and Hs00174944_m1 (*hDIO1*) and purchased from Life Technologies. Diluted cDNA were amplified using the following conditions: 50 C for 2 min, 95 C for 10 min, and 40 cycles of 95 C for 15 sec and 60 C for 1 min, followed by continuous incubation at 25 C. Expression levels of FOXA1, FOXA2, and hDIO1 were normalized to cyclophilin A to compensate for variations in input RNA.

Preparation of cell extracts and EMSA

Nuclear extracts were prepared from HepG2 cells using the Nuclear Extract kit (Active Motif, Carlsbad, CA), according to the manufacturer's instruction. EMSA were conducted using a LightShift chemiluminescent EMSA kit (Thermo Fisher Scientific, Rockford, IL) with slight modifications of the original manufacturer's instruction. Oligonucleotides 3′-end labeled with biotin were synthesized (Life Technologies) and annealed to generate double-stranded oligonucleotide probes. Two hundred femtomoles of oligonucleotide probe were incubated with 10–15 μg of nuclear protein and 0.5 μg of poly (dI-dC) in the presence or absence of competing oligonucleotide in 10× binding buffer [containing 100 mM Tris, 500 mM KCl, and 10 mM dithiothreitol (pH 7.5)] and 75 mM KCl, and 5% glycerol was added to solutions containing probes with an E-box element. After a 30-min incubation at room temperature, DNA-protein complexes were separated by electrophoresis on a 6% DNA retardation gel (Life Technologies) at 4 C in 0.5× Tris-borate, EDTA buffer [containing 89 mM Tris-borate and 2 mM EDTA (pH 8.0)]. For supershift assays, binding reactions were incubated for 45 min at room temperature with antibodies before the addition of labeled probes. The antibodies used in the supershift assays were as follows: 1 μl (200 μg/0.1 ml) of USF1 (sc-8983X), USF2 (sc-861X), E47 (sc-763X), FOXA1 (sc-6553X), FOXA2 (sc-6554X), and FOXA3 (sc-5361X) and 5 μl (200 μg/0.5 ml) of normal goat and normal rabbit IgG, and all were purchased from Santa Cruz Biotechnology, Inc. (Santa Cruz, CA). After electrophoresis, samples were transferred onto nylon membranes and fixed by UV irradiation. Biotinylated DNA was detected using a Fujix Lumino-image analyzer (LAS-1000; Fuji Photo Film Co., Ltd., Tokyo, Japan).

Transfection of short interfering RNA (siRNA)

An aliquot of 6 pmol siRNA specific for FOXA1 and/or FOXA2 (Stealth Select RNAi, Life Technologies) or a negative control siRNA (Stealth RNAi Negative Control, Life Technologies) was transfected into HepG2 cells using the Lipofectamine RNAiMax reagent (Life Technologies) by reverse transfection according to the manufacturer's instruction. After transfection, HepG2 cells were plated at 1.5–2 × 10^5 cells/well in 24-well tissue culture plates and maintained in 0.5 ml of antibiotic-free medium for 24–48 h. mRNA extraction and analysis were performed as described above.

Statistics

The data represent the mean ± SEM and were obtained from at least three separate experiments, each performed in triplicate. Statistical analyses were performed to examine the significance of differences among the results using unpaired *t* test or ANOVA followed by Student-Newman-Keuls test or Dunnett's test.

Results

Functional analysis of the 5′-flanking region of the *hDIO1* gene

To identify regions within the promoter region of *hDIO1* important for regulating its expression, a series of 5′-deletion constructs was subcloned into the pGL4.10 vector and transiently transfected into HepG2 and TSA 201 cells (Fig. 1A). In both HepG2 and TSA 201 cells, luciferase activity increased by deletion of nucleotides −150 to −131 and decreased after deletion of −131 to −103. Among the tested constructs, the luciferase activity produced by transfection of −150/−4 hDIO1-Luc was specifically and markedly decreased in HepG2 cells. Additionally, more pronounced differences were seen between the activity of −150/−4 hDIO1-Luc and −131/−4 hDIO1-Luc in HepG2 cells compared with TSA 201 cells. In addition, luciferase activity was markedly increased by deleting the region from −343 to −187 and decreased after deletion of −187 to −150 only in HepG2 cells. Taken together, these results indicate that the region between nucleotides −187 and −132 is important for *hDIO1* promoter function in HepG2 cells. To confirm the expression of *hDIO1*, we performed RT-PCR using total RNA isolated from HepG2 and TSA 201 cells, a liver and kidney cell line, respectively. As shown in Fig. 1B, although there was a difference in the degree of gene expression, *hDIO1* was expressed in both cell lines; this was consistent with a previous report examining *hDIO1* tissue distribution (2). Additionally, multiple PCR products were detected, because there are several alternative splice variants of *hDIO1* (7). These results indicate that there may exist a sequence

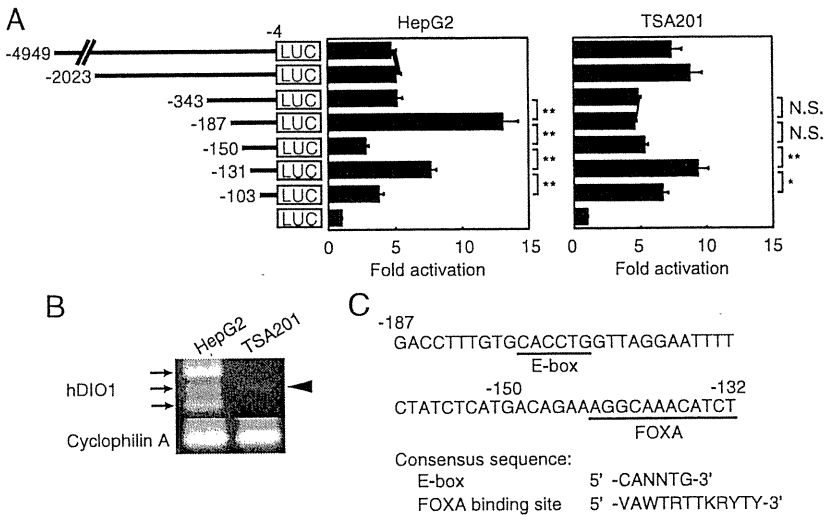

FIG. 1. Liver-specific changes in *hDIO1* promoter activity. A, A series of 5′-deletion constructs of the *hDIO1* promoter were transiently transfected into HepG2 or TSA 201 cells. Promoter activity was normalized to *Renilla* luciferase activity and expressed as the relative activity to promoterless pGL4.10. Statistical significance was determined by ANOVA followed by Student-Newman-Keuls test. *, $P < 0.05$; **, $P < 0.01$. N.S., Not significant. B, RT-PCR analysis of *hDIO1* expression. Electrophoretic analysis of RT-PCR products using total RNA from HepG2 and TSA 201 cells was performed. The *arrows* and *arrowhead* correspond to the RT-PCR products using total RNA from HepG2 and TSA 201 cells, respectively. Cyclophilin A was used as a positive control. C, The nucleotide sequences of the 5′-flanking region of *hDIO1* are shown. The translational start site was set at +1. *Underlined sequences* indicate putative binding sites for transcription factors. Consensus sequences of E-box site and FOXA binding site are shown at the *bottom*. Abbreviations for nucleotides: W (A or T), K (G or T), Y (C or T), R (A or G), V (A, C, or G), and N (A, C, G, or T). LUC, Luciferase.

essential for liver-specific expression of *hDIO1* within the −187 to −132 region of its promoter. A computational analysis of this region revealed the presence of a consensus E-box site between nucleotides −187 and −151 and a FOXA binding site between nucleotides −150 and −132 (Fig. 1C).

Promoter activity associated with the FOXA binding site and the E-box

To better understand the contribution of the FOXA binding site and the E-box on the expression of *hDIO1* in liver-derived HepG2 cells, we examined luciferase activity in cells transfected with wild-type (WT) or mutated *hDIO1* promoter constructs. In HepG2 cells, luciferase activity was increased 2-fold by mutating the FOXA binding site when cells were transfected with a −150/−4 hDIO1-Luc construct (Fig. 2A). In addition, when cells were transfected with a −187/−4 hDIO1-Luc construct, luciferase activity was nearly completely lost by destruction of the E-box, and mutation of the FOXA binding site caused a decrease in luciferase activity by 50% (Fig. 2B). In TSA 201 cells transfected with −187/−4 hDIO1-Luc, luciferase activity was almost completely abolished by mutation of the E-box, but mutation of the FOXA binding site in both −187/−4 hDIO1-Luc and −150/−4 hDIO1-Luc did not significantly affect luciferase activity (Fig. 2). Thus, the E-box present within the *hDIO1* promoter is required for the enhancer activity in both liver- and kidney-derived cells, but the FOXA binding site exhibits liver-specific enhancer and repressor activity.

Binding of FOXA1/FOXA2 to the FOXA binding site and USF to the E-box

To determine the transcription factors that bind to these elements in the promoter of *hDIO1* in HepG2 cells, we performed EMSA using oligonucleotides with the FOXA binding site and the E-box. Incubation of HepG2 cell extracts with oligonucleotides containing the FOXA binding site (Fig. 3A, WT-F) led to the formation of several DNA/protein complexes (Fig. 3B, lane 2). Formation of one of these complexes was inhibited by incubation with excess WT-F, but not mutated oligonucleotide (MUT)-F, demonstrating the specificity of this complex (Fig. 3B, lanes 3–6). Additionally, the complex was supershifted by addition of anti-FOXA1 and anti-FOXA2 antibodies (Fig. 3B, lanes 7 and 8). However, an antibody specific for FOXA3, which binds an identical sequence, or normal goat IgG did not disrupt complex formation (Fig. 3B, lanes 9 and 10). These results suggest that the putative FOXA binding site is specifically bound by FOXA1 or FOXA2. We next examined binding to the E-box sequence, and several complexes were formed by

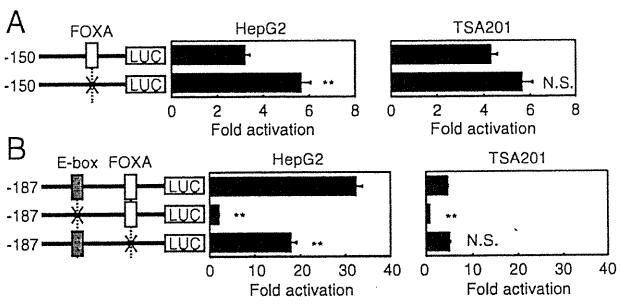

FIG. 2. Changes in *hDIO1* promoter activity by FOXA binding site and E-box. Schematic diagram in the *left* of each figure representing WT and site-specific mutations of the *hDIO1* promoter, introduced into the upstream region of the luciferase gene. A *cross* represents the site-specific mutation of the putative FOXA binding site or E-box. Each construct was transiently transfected into HepG2 or TSA 201 cells. Promoter activity was normalized to *Renilla* luciferase activity and expressed as the relative activity to promoterless pGL4.10. Statistical significance was determined by unpaired *t* test (A) or ANOVA followed by Dunnett's test (B). **, $P < 0.01$. N.S., Not significant.

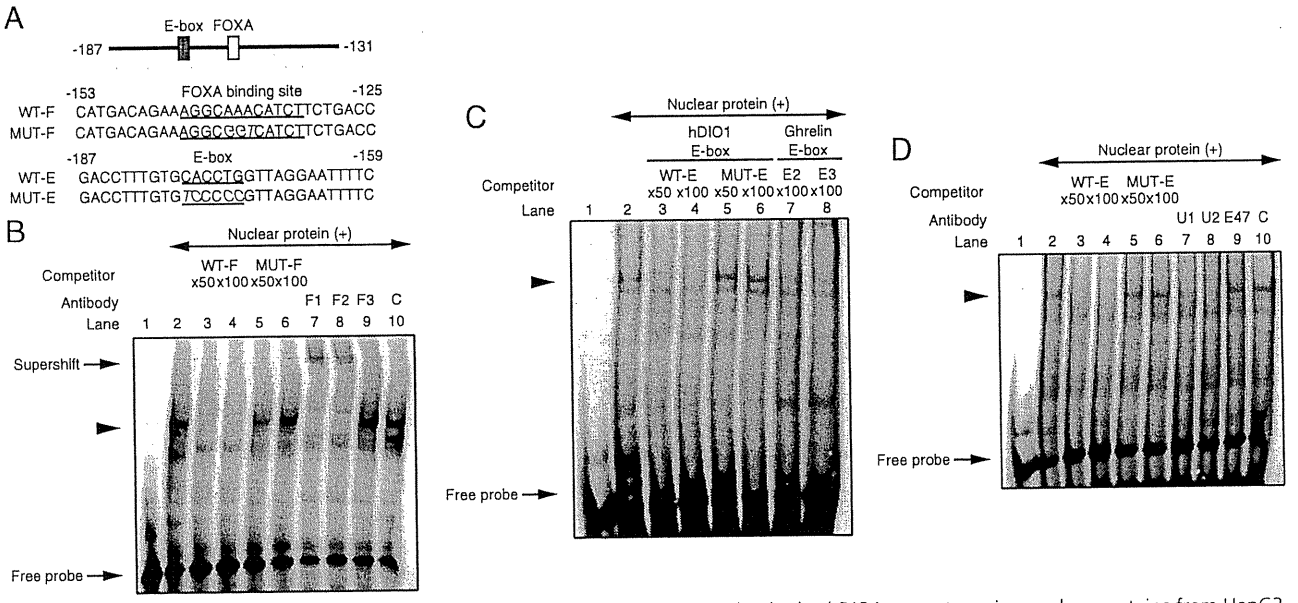

FIG. 3. Specific binding of the transcription factors within the −187 and −132 region in the *hDIO1* promoter using nuclear proteins from HepG2 cells. Panel A, Sequences of the double-stranded oligonucleotides used in EMSA. WT-F, WT *hDIO1* sequence identical to the −153 to −125 region, containing the FOXA binding site at −143 to −132. MUT-F contains a mutated FOXA binding site. WT-E, WT *hDIO1* sequence identical to the −187 to −159 region, containing the E-box at −177 to −172. MUT-E contains a mutated E-box. Each putative binding site is *underlined*; the mutated base pairs are indicated by *italic letters*. Panel B, Oligonucleotide WT-F was used as the probe for EMSA either without competitor (lane 2) or in the presence of 50- and 100-fold molar excesses of unlabeled WT-F (lanes 3 and 4, respectively) or MUT-F (lanes 5 and 6, respectively). The specific complex formed from HepG2 cell nuclear extract and WT-F is indicated by an *arrowhead*. Supershift assay experiments were performed using antibody against FOXA1 (F1; lane 7), FOXA2 (F2; lane 8), or FOXA3 (F3; lane 9) and normal goat IgG (C; lane 10). Panel C, Oligonucleotide WT-E was used as the probe for EMSA either without competitor (lane 2) or in the presence of 50- and 100-fold molar excesses of unlabeled WT-E (lanes 3 and 4, respectively), MUT-E (lanes 5 and 6, respectively), or 100-fold molar excesses of unlabeled E-box from the human ghrelin gene [E2 and E3 (in Ref. 8); lanes 7 and 8, respectively]. The specific complex formed from HepG2 cell nuclear extract and WT-E is indicated by an *arrowhead*. D, Supershift assay experiments were performed using antibody against USF1 (U1; lane 7), USF2 (U2; lane 8), or E47 (E47; lane 9) and normal rabbit IgG (C; lane 10). C, Negative control (normal goat and normal rabbit IgG).

incubation of HepG2 cell extracts with an appropriate oligonucleotide (Fig. 3A, WT-E, and C, lane 2). Formation of one of these complexes was inhibited by incubating with an excess of WT-E and the E-box from human ghrelin gene (8) but not by a mutant oligonucleotide MUT-E (Fig. 3C, lanes 3–8). Computational analysis predicted that the putative E-box site binds the basic/helix-loop-helix-leucine zipper transcription factor USF, and to investigate this hypothesis, a supershift assay was performed using antibodies specific for USF1 and USF2. Addition of antibodies specific for USF1 and USF2 completely inhibited complex formation (Fig. 3D, lanes 7 and 8). However, incubation with an antibody against E47, a protein that binds a similar E-box sequence, or normal rabbit IgG did not disrupt complex formation (Fig. 3D, lanes 9 and 10). These results suggest that USF1/USF2 bind the putative E-box, and this complex likely contains a USF1/USF2 heterodimer. Collectively, FOXA1, FOXA2, and USF likely participate in the regulation of *hDIO1* expression.

Effect of overexpression of FOXA2 or USF on *hDIO1* promoter activity

To determine whether FOXA and USF have the potential to affect the activity of the *hDIO1* promoter in liver cells, a −187/−4 hDIO1-Luc construct was transiently transfected into HepG2 cells along with increasing amounts of either a FOXA2 or USF expression plasmid. The luciferase activity decreased in a dose-dependent manner by cotransfection of the FOXA2 expression plasmid with −187/−4 hDIO1-Luc (Fig. 4A). In contrast, luciferase activity increased dose dependently by the cotransfection of the USF1 or USF2 expression plasmid, and overexpression of USF2 consistently led to greater *hDIO1* promoter activity than expression of USF1 alone (Fig. 4B). Thus, transcription of *hDIO1* is negatively regulated by FOXA2 and positively regulated by USF. Although we transiently transfected a −187/−4 hDIO1-Luc construct into HepG2 cells along with increasing amounts of a FOXA1 expression plasmid, we could not obtain appropriate data, indicating that the FOXA1 expression plasmid we used did not function in our experimental system for unknown reason.

RNA interference

Next, we determined the effects of FOXA on the native *hDIO1* promoter using siRNA-mediated knockdown of FOXA in HepG2 cells. As shown in Fig. 5, A and B, knock-

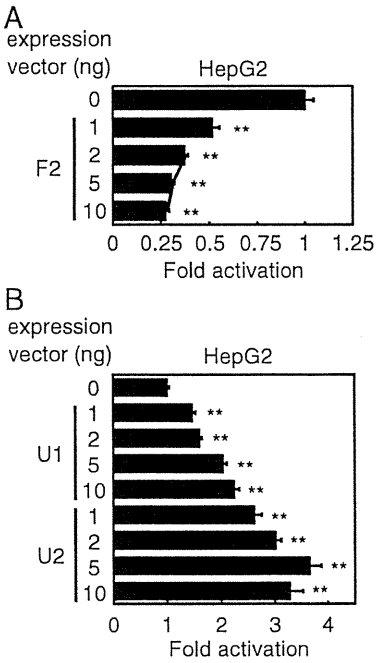

FIG. 4. Effect of overexpression of FOXA2 or USF on *hDIO1* promoter activity. −187/−4 hDIO1-Luc was transiently transfected into HepG2 cells in the presence of increasing amounts of vectors expressing FOXA2 (F2) (A) or USF1 or USF2 (U1 and U2, respectively) (B). Promoter activity was normalized to *Renilla* luciferase activity, then expressed as the relative activity to −187/−4 hDIO1-Luc cotransfected with pF4A without a cDNA insert. Statistical significance was determined by ANOVA followed by Dunnett's test. **, $P < 0.01$.

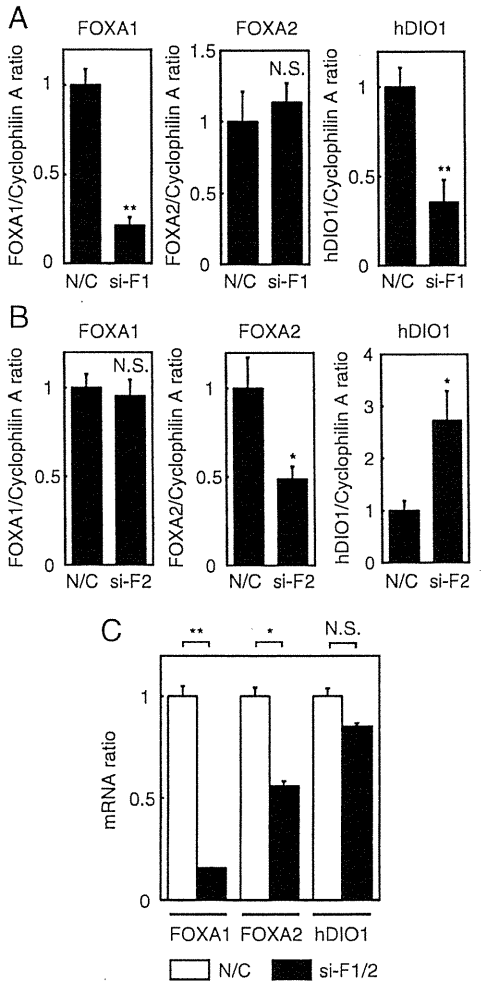

FIG. 5. Knockdown of FOXA1 and/or FOXA2. Effect of transfection of FOXA1 (A) and FOXA2 (B) siRNA on the mRNA expression level of FOXA1, FOXA2, and D1. Simultaneous knockdown of FOXA1 and FOXA2 (C) was performed using siRNA that has identical sequences in both FOXA1 and FOXA2. N/C, Negative control siRNA; si-F1, siRNA specific for FOXA1; si-F2, siRNA specific for FOXA2; si-F1/2, siRNA specific for both FOXA1 and FOXA2. mRNA expression level was normalized to that of cyclophilin A in each sample and expressed as the relative activity to the basal expression (N/C). Statistical significance was determined by unpaired *t* test. *, $P < 0.05$; **, $P < 0.01$. N.S., Not significant.

down of FOXA1 decreased the expression of *hDIO1* mRNA, and knockdown of FOXA2 increased the expression level of *hDIO1* mRNA. FOXA1 and FOXA2 did not affect each other's expression by knockdown of them (Fig. 5, A and B). In addition, when both FOXA1 and FOXA2 were knocked down simultaneously, no change in the expression of *hDIO1* mRNA was seen (Fig. 5C). Thus, *hDIO1* expression is positively regulated by FOXA1 and negatively regulated by FOXA2, and FOXA1 and FOXA2 interact with each other to regulate *hDIO1* expression.

Interaction between FOXA and USF in the activation of the *hDIO1* promoter

Transcription factors frequently interact to coordinately regulate gene expression, and we first wished to determine whether the FOXA binding site and the E-box present in the *hDIO1* promoter interact. We cotransfected a WT or mutated −187/−4 hDIO1-Luc construct and USF expression plasmids into HepG2 cells. When the FOXA binding site was mutated, the transcription activity of the *hDIO1* promoter in the presence of transfected USF was attenuated (Fig. 6A). Thus, activation of the *hDIO1* promoter by USF depends on the presence of a functional FOXA binding site. Next, we investigated the effects of FOXA on the response of the *hDIO1* promoter to USF.

We knocked down the expression of FOXA and cotransfected a −187/−4 hDIO1-Luc construct along with USF expression plasmids into HepG2 cells. As shown in Fig. 6B, the transcription activity of the *hDIO1* promoter was attenuated by knockdown of FOXA1 and enhanced by knockdown of FOXA2. The transcription activity of the *hDIO1* promoter was also attenuated by simultaneous knockdown of FOXA1 and FOXA2 to an extent similar to that seen for the knockdown of FOXA1. The suppressed activity by knockdown of FOXA1 was not restored by overexpression of USF, and the enhanced activity by knockdown of FOXA2 was further enhanced by overexpression of USF. Thus, the response of the *hDIO1* pro-

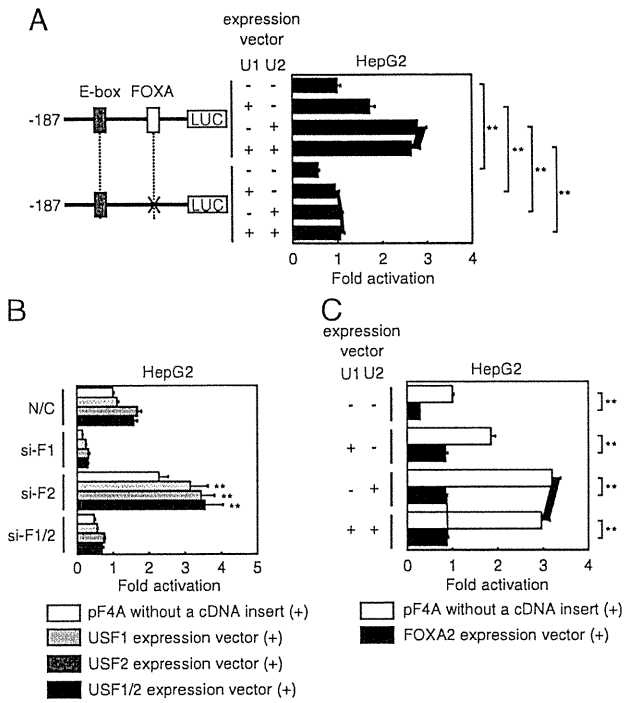

FIG. 6. Interaction between FOXA and USF in the activation of the *hDIO1* promoter. A, Dependence of the activation of *hDIO1* promoter by USF on the FOXA binding site. Schematic diagram in the *left* of figure representing WT and site-specific mutations of the *hDIO1* promoter, introduced into the upstream region of the luciferase gene. A *cross* represents the site-specific mutation of the putative FOXA binding site. Each construct was transiently cotransfected into HepG2 cells in the presence of 5 ng of vectors expressing USF1 (U1) and/or USF2 (U2). Promoter activity was normalized to *Renilla* luciferase activity, then expressed as the relative activity to −187/−4 hDIO1-Luc cotransfected with pF4A without a cDNA insert. Statistical significance was determined by ANOVA followed by Student-Newman-Keuls test. **, $P < 0.01$. B, Effect of knockdown of FOXA on the activation of the *hDIO1* promoter by USF. Short interfering RNA specific for FOXA1 and/or FOXA2 or a negative control siRNA were transfected into HepG2 cells as described in *Materials and Methods*. One day after siRNA transfection, −187/−4 hDIO1-Luc was transiently cotransfected in the presence of 5 ng of vectors expressing USF1 and/or USF2. N/C, Negative control siRNA; si-F1, siRNA specific for FOXA1; si-F2, siRNA specific for FOXA2; si-F1/2, siRNA specific for both FOXA1 and FOXA2. Promoter activity was normalized to *Renilla* luciferase activity, then expressed as the relative activity to −187/−4 hDIO1-Luc cotransfected with pF4A without a cDNA insert after knockdown by negative control siRNA. Statistical significance was determined by ANOVA followed by Student-Newman-Keuls test. **, $P < 0.01$ relative to −187/−4 hDIO1-Luc cotransfected with pF4A without a cDNA insert after knockdown by siRNA specific for FOXA2. C, Effect of overexpression of FOXA2 on the activation of the *hDIO1* promoter by USF. −187/−4 hDIO1-Luc was transiently transfected into HepG2 cells in the presence of 5 ng of vectors expressing USF1 (U1), USF2 (U2), and/or FOXA2. Promoter activity was normalized to *Renilla* luciferase activity, then expressed as the relative activity to −187/−4 hDIO1-Luc cotransfected with pF4A without a cDNA insert. Statistical significance was determined by ANOVA followed by Student-Newman-Keuls test. **, $P < 0.01$. LUC, Luciferase.

moter to USF was greatly attenuated by knockdown of FOXA1 and enhanced by knockdown of FOXA2. Furthermore, we cotransfected a −187/−4 hDIO1-Luc construct and USF expression plasmids with or without a FOXA2 expression plasmid into HepG2 cells. The transcription activity of the *hDIO1* promoter was enhanced in the presence of transfected USF (Fig. 6C, *white bar*), but the activity was greatly attenuated by cotransfection of the FOXA2 expression plasmid (Fig. 6C, *black bar*). Thus, the response of the *hDIO1* promoter to USF was attenuated by the coexpression of FOXA2. Collectively, these results indicate that FOXA1 is required for the activation of the *hDIO1* promoter by USF and that FOXA2 represses the transcription of *hDIO1* and disrupts the interaction of USF with FOXA1 by occupying the FOXA binding site.

Discussion

In this study, we analyzed the 5′-upstream region of *hDIO1* to identify protein-DNA interactions within the *hDIO1* promoter. Our experiments demonstrated that the region between nucleotides −187 and −132 is important for *hDIO1* promoter activity in HepG2 cells. We identified functional elements for FOXA and USF within this region, and we showed that these sites are important for the transcriptional regulation of *hDIO1*. Recently, Ohguchi *et al.* (9) identified a proximal hepatocyte nuclear factor (HNF)4α binding site in mice, and they demonstrated that the HNF4α binding site is essential for the activation of the mouse D1 gene by HNF4α. Deletion analyses of the 5′-flanking region of *hDIO1* were performed by Jakobs *et al.* (10) by transfecting 1.5- and 0.1-kb constructs into HepG2 cells, and they found that both constructs substantially increased luciferase activity compared with a promoterless vector. However, they did not perform a higher resolution promoter analysis, and we are the first to identify functional elements other than thyroid hormone responsive element in the *hDIO1* promoter.

The FOXA proteins were first identified as liver-enriched factors because of their ability to bind the transthyretin gene promoter, and they were originally termed HNF3 (11). There are three FOXA proteins, FOXA1 (HNF3α), FOXA2 (HNF3β), and FOXA3 (HNF3γ), which are encoded by different genes on different chromosomes (12). FOXA proteins play important roles in early embryonic development and organogenesis, and they are recognized as "pioneer factors" (13). In addition, the FOXA proteins control glucose metabolism through the regulation of multiple target genes in the liver, pancreas, and adipose tissue after birth (13). Our EMSA experiments demonstrated that FOXA1 and FOXA2 specifically bound the identical FOXA binding site of the *hDIO1* promoter. Although all three FOXA proteins exist relatively abundant in HepG2 cells (14) and recognize the same DNA sequences, slight differences in the binding affin-

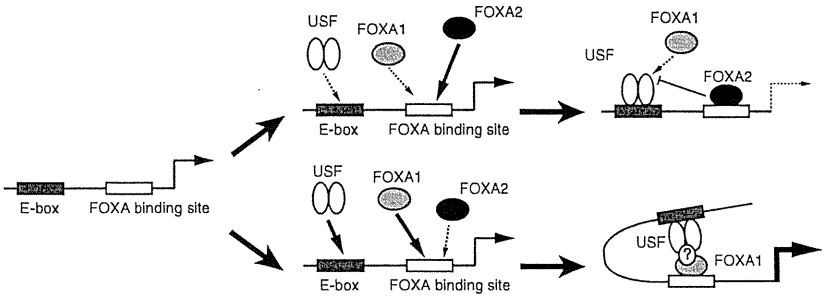

FIG. 7. A model for the regulation of liver-specific expression of *hDIO1* by FOXA1, FOXA2, and USF. FOXA1 and FOXA2 bind and share the identical FOXA binding site, and USF binds the E-box as a heterodimer. FOXA2 represses the transcription of *hDIO1* through the FOXA binding site (*upper panel*), and FOXA1 and USF work cooperatively to activate *hDIO1* transcription (*lower panel*).

ity and DNA binding capacity may account for their specificity (15). Indeed, there are very few reports that FOXA1 and FOXA2 share an identical binding site and coparticipate in the transcriptional regulation of a single gene (16). Our transfection assays and siRNA experiments demonstrated that *hDIO1* is positively regulated by FOXA1 and negatively regulated by FOXA2 and that FOXA1 and FOXA2 interact to coordinately regulate *hDIO1* expression. These results suggest that FOXA proteins are involved in thyroid hormone homeostasis.

USF proteins were first identified as regulators of adenovirus major late promoter transcription (17, 18). There are two USF proteins, 43 kDa (USF1) and 44 kDa (USF2), encoded by different genes on different chromosomes (19, 20). USF proteins primarily bind as dimers to consensus sequences containing the CACGTG motif termed an E-box (18, 19, 21). USF proteins are ubiquitously expressed, although different ratios of USF homo- and heterodimers are found in different cell types (22). The molecular details of USF binding and activity have been well characterized, but its biological role remains poorly understood. USF proteins regulate the expression of several genes related to glucose and lipid metabolism and peptide hormone synthesis, including liver-type pyruvate kinase (23) and glucokinase (24), fatty acid synthase (25), apolipoprotein A-II (26), calcitonin/calcitonin gene-related peptide (27), and ghrelin (8). In our study, we demonstrated that the putative E-box site in the *hDIO1* promoter specifically bound the USF1/USF2 heterodimer and that promoter activity increased in a dose-dependent manner with the cotransfection of the USF1/2 expression plasmid. These results suggest that USF positively regulate *hDIO1* expression. Additionally, promoter activity was almost completely abolished by mutation of the E-box motif, indicating that USF proteins are critical for the transcriptional regulation of *hDIO1* and thyroid hormone homeostasis in the liver and possibly kidney.

The response of the *hDIO1* promoter to USF was greatly attenuated by mutation of the FOXA binding site or knockdown of FOXA1, indicating that FOXA1 is necessary for the expression of *hDIO1* by USF. FOXA1 plays an essential role in the "pioneering" of gene regulatory elements, allowing for the recruitment of additional factors required for gene regulation (28), and our data suggest that USF cooperates with FOXA1 to regulate *hDIO1* promoter activity. Although we could not confirm the interaction between FOXA1 with USF by coimmunoprecipitation experiments in our experimental condition (data not shown), a direct physical interaction between FOXA1 and USF has been reported through the use of immunoprecipitation and glutathione *S*-transferase pull-down assays (29). Furthermore, the cooperation between FOXA1 and USF likely contributes to the liver-specific activation of *hDIO1*; although FOXA1 was expressed in both HepG2 and TSA201 cells in our preliminary experiments (data not shown), only HepG2 cells demonstrated substantial differences in promoter activity by transfection of −187/−4 hDIO1-Luc and mutation of the FOXA binding site. Interactions between cell-specific factors and other regulators are thought to contribute to the tissue-specific control of gene expression by the ubiquitous USF proteins (26, 30–34), and Fig. 7 shows our working model for the regulation of liver-specific expression of *hDIO1* by transcription factor binding to the −187 to −132 region of the *hDIO1* promoter. In this model, *hDIO1* promoter activity is modulated by FOXA1, FOXA2, and USF proteins, and these transcription factors interact with each other to fine-tune the *hDIO1* promoter activity.

In conclusion, we have shown that FOXA1, FOXA2, and USF regulate *hDIO1* expression in the liver. FOXA1 and FOXA2 both participate in the liver-specific regulation of *hDIO1* expression, and FOXA1 and USF act together to promote the liver-specific activation of *hDIO1*. FOXA1 and FOXA2 are likely involved in thyroid hormone homeostasis in the liver.

Acknowledgments

We thank Mami Yoshida and Yudai Takeuchi for technical assistance and Miyuki Ban for secretarial assistance.

Address all correspondence and requests for reprints to: Naotetsu Kanamoto, M.D., Ph.D., Department of Medicine and Clinical Science, Kyoto University Graduate School of Medicine, 54 Shogoin Kawahara-cho, Sakyo-ku, Kyoto 606-8507, Japan. E-mail: kyotetsu@kuhp.kyoto-u.ac.jp.

This work was supported by a Grant-in-Aid for Scientific Research from the Ministry of Health, the Labor and Welfare of Japan, Ministry of Education, Culture, Sports, Sciences, and Technology of Japan Grants 18790635, 19591075, and 21119013, and the Takeda Science Foundation.

Disclosure Summary: The authors have nothing to disclose.

References

1. Bianco AC, Salvatore D, Gereben B, Berry MJ, Larsen PR 2002 Biochemistry, cellular and molecular biology, and physiological roles of the iodothyronine selenodeiodinases. Endocr Rev 23:38–89
2. Berry MJ, Banu L, Larsen PR 1991 Type I iodothyronine deiodinase is a selenocysteine-containing enzyme. Nature 349:438–440
3. Toyoda N, Zavacki AM, Maia AL, Harney JW, Larsen PR 1995 A novel retinoid X receptor-independent thyroid hormone response element is present in the human type 1 deiodinase gene. Mol Cell Biol 15:5100–5112
4. Nagaya T, Fujieda M, Otsuka G, Yang JP, Okamoto T, Seo H 2000 A potential role of activated NF-κB in the pathogenesis of euthyroid sick syndrome. J Clin Invest 106:393–402
5. Moriyama K, Tagami T, Akamizu T, Usui T, Saijo M, Kanamoto N, Hataya Y, Shimatsu A, Kuzuya H, Nakao K 2002 Thyroid hormone action is disrupted by bisphenol A as an antagonist. J Clin Endocrinol Metab 87:5185–5190
6. Heinemeyer T, Wingender E, Reuter I, Hermjakob H, Kel AE, Kel OV, Ignatieva EV, Ananko EA, Podkolodnaya OA, Kolpakov FA, Podkolodny NL, Kolchanov NA 1998 Databases on transcriptional regulation: TRANSFAC, TRRD and COMPEL. Nucleic Acids Res 26:362–367
7. Piekielko-Witkowska A, Master A, Wojcicka A, Boguslawska J, Brozda I, Tanski Z, Nauman A 2009 Disturbed expression of type 1 iodothyronine deiodinase splice variants in human renal cancer. Thyroid 19:1105–1113
8. Kanamoto N, Akamizu T, Tagami T, Hataya Y, Moriyama K, Takaya K, Hosoda H, Kojima M, Kangawa K, Nakao K 2004 Genomic structure and characterization of the 5′-flanking region of the human ghrelin gene. Endocrinology 145:4144–4153
9. Ohguchi H, Tanaka T, Uchida A, Magoori K, Kudo H, Kim I, Daigo K, Sakakibara I, Okamura M, Harigae H, Sasaki T, Osborne TF, Gonzalez FJ, Hamakubo T, Kodama T, Sakai J 2008 Hepatocyte nuclear factor 4α contributes to thyroid hormone homeostasis by cooperatively regulating the type 1 iodothyronine deiodinase gene with GATA4 and Kruppel-like transcription factor 9. Mol Cell Biol 28:3917–3931
10. Jakobs TC, Schmutzler C, Meissner J, Köhrle J 1997 The promoter of the human type I 5′-deiodinase gene—mapping of the transcription start site and identification of a DR+4 thyroid-hormone-responsive element. Eur J Biochem 247:288–297
11. Lai E, Prezioso VR, Smith E, Litvin O, Costa RH, Darnell JE Jr 1990 HNF-3A, a hepatocyte-enriched transcription factor of novel structure is regulated transcriptionally. Genes Dev 4:1427–1436
12. Kaestner KH, Hiemisch H, Luckow B, Schütz G 1994 The HNF-3 gene family of transcription factors in mice: gene structure, cDNA sequence, and mRNA distribution. Genomics 20:377–385
13. Friedman JR, Kaestner KH 2006 The Foxa family of transcription factors in development and metabolism. Cell Mol Life Sci 63:2317–2328
14. Motallebipour M, Ameur A, Reddy Bysani MS, Patra K, Wallerman O, Mangion J, Barker MA, McKernan KJ, Komorowski J, Wadelius C 2009 Differential binding and co-binding pattern of FOXA1 and FOXA3 and their relation to H3K4me3 in HepG2 cells revealed by ChIP-seq. Genome Biol 10:R129
15. Yu X, Gupta A, Wang Y, Suzuki K, Mirosevich J, Orgebin-Crist MC, Matusik RJ 2005 Foxa1 and Foxa2 interact with the androgen receptor to regulate prostate and epididymal genes differentially. Ann NY Acad Sci 1061:77–93
16. Shimizu S, Miyamoto Y, Hayashi M 2002 Cell-type dependency of two Foxa/HNF3 sites in the regulation of vitronectin promoter activity. Biochim Biophys Acta 1574:337–344
17. Miyamoto NG, Moncollin V, Egly JM, Chambon P 1985 Specific interaction between a transcription factor and the upstream element of the adenovirus-2 major late promoter. EMBO J 4:3563–3570
18. Sawadogo M, Roeder RG 1985 Interaction of a gene-specific transcription factor with the adenovirus major late promoter upstream of the TATA box region. Cell 43:165–175
19. Gregor PD, Sawadogo M, Roeder RG 1990 The adenovirus major late transcription factor USF is a member of the helix-loop-helix group of regulatory proteins and binds to DNA as a dimer. Genes Dev 4:1730–1740
20. Sawadogo M, Van Dyke MW, Gregor PD, Roeder RG 1988 Multiple forms of the human gene-specific transcription factor USF. I. Complete purification and identification of USF from HeLa cell nuclei. J Biol Chem 263:11985–11993
21. Bendall AJ, Molloy PL 1994 Base preferences for DNA binding by the bHLH-Zip protein USF: effects of MgCl2 on specificity and comparison with binding of Myc family members. Nucleic Acids Res 22:2801–2810
22. Sirito M, Lin Q, Maity T, Sawadogo M 1994 Ubiquitous expression of the 43- and 44-kDa forms of transcription factor USF in mammalian cells. Nucleic Acids Res 22:427–433
23. Vallet VS, Casado M, Henrion AA, Bucchini D, Raymondjean M, Kahn A, Vaulont S 1998 Differential roles of upstream stimulatory factors 1 and 2 in the transcriptional response of liver genes to glucose. J Biol Chem 273:20175–20179
24. Iynedjian PB 1998 Identification of upstream stimulatory factor as transcriptional activator of the liver promoter of the glucokinase gene. Biochem J 333(Pt 3):705–712
25. Casado M, Vallet VS, Kahn A, Vaulont S 1999 Essential role in vivo of upstream stimulatory factors for a normal dietary response of the fatty acid synthase gene in the liver. J Biol Chem 274:2009–2013
26. Ribeiro A, Pastier D, Kardassis D, Chambaz J, Cardot P 1999 Cooperative binding of upstream stimulatory factor and hepatic nuclear factor 4 drives the transcription of the human apolipoprotein A-II gene. J Biol Chem 274:1216–1225
27. Lanigan TM, Russo AF 1997 Binding of upstream stimulatory factor and a cell-specific activator to the calcitonin/calcitonin gene-related peptide enhancer. J Biol Chem 272:18316–18324
28. Cirillo LA, McPherson CE, Bossard P, Stevens K, Cherian S, Shim EY, Clark KL, Burley SK, Zaret KS 1998 Binding of the winged-helix transcription factor HNF3 to a linker histone site on the nucleosome. EMBO J 17:244–254
29. Sun Q, Yu X, Degraff DJ, Matusik RJ 2009 Upstream stimulatory factor 2, a novel FoxA1-interacting protein, is involved in prostate-specific gene expression. Mol Endocrinol 23:2038–2047
30. Greenall A, Willingham N, Cheung E, Boam DS, Sharrocks AD 2001 DNA binding by the ETS-domain transcription factor PEA3 is regulated by intramolecular and intermolecular protein.protein interactions. J Biol Chem 276:16207–16215
31. Heckert LL 2001 Activation of the rat follicle-stimulating hormone receptor promoter by steroidogenic factor 1 is blocked by protein kinase a and requires upstream stimulatory factor binding to a proximal E box element. Mol Endocrinol 15:704–715
32. Ismail PM, Lu T, Sawadogo M 1999 Loss of USF transcriptional activity in breast cancer cell lines. Oncogene 18:5582–5591
33. Martin CC, Svitek CA, Oeser JK, Henderson E, Stein R, O'Brien RM 2003 Upstream stimulatory factor (USF) and neurogenic differentiation/β-cell E box transactivator 2 (NeuroD/BETA2) contribute to islet-specific glucose-6-phosphatase catalytic-subunit-related protein (IGRP) gene expression. Biochem J 371:675–686
34. Qyang Y, Luo X, Lu T, Ismail PM, Krylov D, Vinson C, Sawadogo M 1999 Cell-type-dependent activity of the ubiquitous transcription factor USF in cellular proliferation and transcriptional activation. Mol Cell Biol 19:1508–1517

the FEBS Journal

MINIREVIEW

Natriuretic peptide system: an overview of studies using genetically engineered animal models

Ichiro Kishimoto[1,2], Takeshi Tokudome[1], Kazuwa Nakao[3] and Kenji Kangawa[1]

1 Department of Biochemistry, National Cerebral and Cardiovascular Center Research Institute, Osaka, Japan
2 Department of Endocrinology and Metabolism, National Cerebral and Cardiovascular Center, Osaka, Japan
3 Department of Medicine and Clinical Science, Kyoto University Graduate School of Medicine, Japan

Keywords
bone; cardiac hypertrophy; guanylyl cyclase; hypertension; natriuretic peptide

Correspondence
I. Kishimoto, Department of Biochemistry, National Cerebral and Cardiovascular Center Research Institute, 5-7-1 Fujishiro-dai, Suita, Osaka 565-8565, Japan
Fax: +81 6 6835 5402
Tel: +81 6 6833 5012
E-mail: kishimot@ri.ncvc.go.jp

(Received 16 August 2010, revised 11 March 2011, accepted 1 April 2011)

doi:10.1111/j.1742-4658.2011.08116.x

The mammalian natriuretic peptide system, consisting of at least three ligands and three receptors, plays critical roles in health and disease. Examination of genetically engineered animal models has suggested the significance of the natriuretic peptide system in cardiovascular, renal and skeletal homeostasis. The present review focuses on the *in vivo* roles of the natriuretic peptide system as demonstrated in transgenic and knockout animal models.

Natriuretic peptides

The existence of an atrial factor with diuretic and natriuretic activities has been postulated since 1981 [1]. In 1983–1984, the isolation and purification of such a factor and determination of its amino acid sequence were accomplished in rats and humans [2–7]. The factor is a peptide distributed mainly in the right and left cardiac atria within granules of myocytes and thus called atrial natriuretic factor or atrial natriuretic peptide (ANP). The discovery of ANP revealed that the heart is not only a mechanical pump driving the circulation of blood but also an endocrine organ regulating the cardiovascular–renal system. For instance, in situations of excessive fluid volume, cardiac ANP secretion is stimulated, which causes vasodilatation, increased renal glomerular filtration and salt/water excretion and inhibition of aldosterone release from the adrenal gland, which collectively result in a reduction of body fluid volume.

Later, in 1988, a homologous peptide with similar biological activities was isolated from porcine brain and hence was named brain natriuretic peptide (BNP) [8]. However, it was soon found that brain BNP levels were much lower in other species. It has since been shown that BNP is mainly produced and secreted by the heart ventricles [9]. Synthesis and secretion of BNP are regulated differently from ANP [10], and the plasma concentration of BNP has been found to reflect the severity of heart failure more closely than ANP [11].

In 1990, yet another type of natriuretic peptide was isolated from porcine brain and named C-type

Abbreviations
ANP, atrial natriuretic peptide; BNP, brain natriuretic peptide; CNP, C-type natriuretic peptide; GC, guanylyl cyclase; MCIP1, myocyte-enriched calcineurin-interacting protein; PAR, protease-activated receptor; PKG, cGMP-dependent protein kinase; RGS, regulator of G-protein signaling.

natriuretic peptide (CNP) [12]. CNP was initially thought to function only in the brain but was later shown to be produced in peripheral tissues such as the vascular endothelium [13] and in smooth muscle cells and macrophages [14]. Because CNP plasma levels are considerably lower than those of ANP or BNP, CNP is thought to mainly act locally as a paracrine factor rather than as a circulating hormone.

Natriuretic peptide receptors

To date, three receptors for natriuretic peptides have been identified. In 1988, one type of ANP receptor was isolated from cultured vascular smooth muscle cells. Using its partial amino acid sequence, the full-length cDNA was cloned and the entire amino acid sequence was deduced [15]. The receptor molecule consists of 496 amino acid residues and contains a large extracellular domain, a putative single transmembrane helix and a 37 amino acid residue cytoplasmic domain. It is generally accepted that the role of this receptor is to bind and remove natriuretic peptides and their fragments from the circulation. Hence, this receptor is termed natriuretic peptide clearance receptor (C receptor). On the other hand, a signaling role of the C receptor has also been suggested [16].

One of the earliest events following the binding of ANP to its receptor is increase in the cytosolic cyclic guanosine monophosphate (cGMP) levels. This finding suggested that cGMP might act as the second messenger mediating the physiological activities of ANP and that the ANP receptor is coupled to guanylyl cyclase (GC), the enzyme that catalyzes the generation of cGMP. In 1989, a segment of the sea urchin GC cDNA was used as a probe to screen various cDNA libraries, which enabled cloning of the first mammalian GC (thus called GC-A) from rats and humans [17]. Expression of the cloned enzyme confirmed that GC-A is an ANP receptor. Soon after the discovery of GC-A, cloning of a second mammalian GC (GC-B) was reported [18,19]. GC-B also bound and was activated by natriuretic peptides, demonstrating the diversity within the natriuretic peptide receptor family. Since these receptor proteins were first identified as GC family members, we refer to them as GC-A or GC-B throughout this paper.

Ligand selectivity

Subsequent studies revealed that GC-A preferentially binds and responds to ANP, while GC-B preferentially responds to CNP [20]. The relative effectiveness of the three natriuretic peptides in stimulating cGMP production via GC-A and GC-B has been reported [21]. The rank order of potency for cGMP production via the GC-A receptor was ANP ≥ BNP > > CNP. On the other hand, cGMP response via GC-B was CNP > ANP or BNP. Thus, the biological functions of natriuretic peptides are mediated by two receptors: GC-A (also known as the A-type natriuretic peptide receptor, NPRA), which is selective for the cardiac peptides ANP and BNP, and GC-B (also called the B-type natriuretic peptide receptor, NPRB), which is selective for CNP.

The binding affinities of ANP, BNP and CNP to the human or rat C receptor have been reported [21]. Irrespective of the species examined, the rank order of affinity for the C receptor was ANP > CNP > BNP. This finding suggests that BNP is the least susceptible to C-receptor-mediated clearance and is more stable in the plasma.

Lessons from genetically engineered animals

A variety of genetically engineered mice have been generated to study the physiological function of each component of the natriuretic peptide–receptor system (summarized in Table 1).

Role of ANP- and BNP-mediated GC-A signaling in blood pressure regulation

Transgenic animals, which constitutively express a fusion gene consisting of the transthyretin promoter and the *ANP* gene, have plasma ANP levels that are higher than non-transgenic littermates by 5–10 fold [22]. The mean arterial pressure in the transgenic animals was reduced by 24 mmHg, which was accompanied by a 27% reduction in total heart weight. This chronic reduction in blood pressure was due to a 21% reduction in total peripheral resistance, whereas cardiac output, stroke volume and heart rate were not significantly altered. In 1994, transgenic mice carrying the human serum amyloid P component/mouse *BNP* fusion gene were generated so that the hormone expression is targeted to the liver [23]. The animals exhibited 10- to 100-fold increase in plasma BNP concentration and significantly lower blood pressure than their non-transgenic littermates.

In 1995, ANP-deficient mice were generated, and their blood pressure phenotype was reported [24]. The mutant mice (homozygous null for the *ANP* gene) had no circulating or atrial ANP, and their blood pressures were significantly higher (8–23 mmHg) than the control mice when they were fed standard diets. When fed

Table 1. Phenotypes of the genetically engineered animals for the natriuretic peptide system.

Mutated gene	Targeting construct	Targeted tissue	Blood pressure phenotype	Cardiac phenotype	Other phenotypes
ANP overexpression [22]	Mouse transthyretin promoter/mouse *ANP* fusion gene	Liver	~ 25 mmHg lower than the control	27% reduction in heart weight	Plasma ANP elevated 8-fold or more; 21% reduction in peripheral resistance
ANP knockout [24]	11 bp in exon-2 replaced with the neomycin resistance gene	Systemic disruption	Increase, 8–23 mmHg (homozygotes); normal on standard diet; 27 mmHg increase on high-salt diet (heterozygotes)	Heart to body weight ratio 1.4-fold higher than the wild-type	Heterozygotes have normal level of circulating ANP
BNP overexpression [23]	Human serum amyloid P component/mouse *BNP* fusion gene	Liver	~ 20 mmHg lower than non-transgenic littermates	~ 30% less heart weight than non-transgenic littermates	10- to 100- fold increase in plasma BNP concentration; skeletal overgrowth
BNP knockout [31]	Exons 1 and 2 replaced with the neomycin resistance gene	Systemic disruption	No signs of systemic hypertension	No signs of ventricular hypertrophy; pressure-overload-induced focal ventricular fibrosis	
CNP overexpression in the cartilage [63]	Col2a1 promoter region/mouse *CNP* fusion gene	Growth plate cartilage	Not reported	Not reported	Longitudinal overgrowth of bones (limbs, vertebrae, skull)
CNP overexpression in the liver [64]	Human serum amyloid P component/mouse *CNP* fusion gene	Liver	Systolic blood pressure unaffected	Heart weight unaffected	Elongation of cartilage bones; plasma CNP level is 84% higher than control
CNP overexpression in the heart [65]	*CNP* gene fused downstream of the murine α-myosin heavy chain promoter	Heart	No change	No change at baseline	Ventricular hypertrophy after myocardial infarction is prevented
CNP knockout (Kyoto) [59]	Exons 1 and 2 encoding CNP replaced with the neomycin resistance gene	Systemic disruption	Not reported	Not reported	Severe dwarfism: impaired endochondral ossification; impaired nociceptive neurons [62]
CNP knockout (Berlin) [66]	Exon 1 replaced with a lacZ expression cassette	Systemic disruption	Not reported	Not reported	Lack of bifurcation of sensory axons in the embryonic dorsal root entry zone
GC-A knock-in overexpression [27]	Entire *GC-A* gene duplicated with the neomycin resistance gene in between	Systemic overexpression	Average 5.2 mmHg below normal in F1 mice carrying three copies of the *GC-A* gene	No effect on heart weights	
GC-A overexpression in the heart [39]	*GC-A* gene fused downstream of murine α-myosin heavy chain promoter	Heart	Normal blood pressure	Heart weight to body weight ratio was significantly less by ~ 15%	

FEBS Journal **278** (2011) 1830–1841 © 2011 The Authors Journal compilation © 2011 FEBS

Table 1. (Continued).

Mutated gene	Targeting construct	Targeted tissue	Blood pressure phenotype	Cardiac phenotype	Other phenotypes
GC-A knockout (Dallas) [25]	Neomycin resistance gene inserted in exon 4, which encodes the transmembrane domain	Systemic disruption	Systolic blood pressure is 20–25 mmHg higher than wild-type	Global cardiac hypertrophy (40–60% increase in heart weight); cardiac contractility similar to that in wild-type mice	Rapid increases in urine output, urinary sodium and cGMP excretion after plasma volume expansion are abolished; increased susceptibility to hypoxia-induced pulmonary hypertension
GC-A knockout (North Carolina) [26]	Exon 1, intron 1 and a portion of exon 2 were replaced with the neomycin resistance gene	Systemic disruption	16 mmHg higher than the control	Heart to body weight ratio averaging185% (male) and 133% (female) of wild-type	Sudden death, with morphological evidence indicative of congestive heart failure or of aortic dissection; resistant to LPS-induced fall in blood pressure
GC-A conditional knockout	Targeting vector contains exons 1–13 and an additional 3.8 kb of the 5′ sequence of the *GC-A* gene, a loxP-flanked neomycin resistance cassette (at −2.6 kb of exon 1) and a third loxP site in the middle of intron 1	Cardiomyocytes (by crossing with cardiac α-myosin heavy chain promoter Cre mice) [43]	7–10 mmHg below normal (due to increased secretion of cardiac natriuretic peptides)	20% increase in heart to body weight ratio compared with floxed GC-A mice; ventricular collagen fractions unaffected; preserved cardiac contractility; decreased cardiac relaxation; markedly impaired cardiac function after pressure overload	~ 2-fold increase in plasma ANP concentration
		Smooth muscle cells (by crossing with SM22-Cre mice) [33]	Normal; acute effect of exogenous ANP on blood pressure abolished	Heart weight and heart to body weight ratio are not different from wild-type	Exaggerated blood pressure response to acute plasma volume expansion; higher vasodilatation sensitivity to nitric oxide and enhanced expression of soluble guanylyl cyclase
		Vascular endothelial cells (by crossing with Tie2 promoter/enhancer Cre mice) [32]	Elevated systolic blood pressure by 12–15 mmHg	~ 20% increase in heart weight	Plasma volume is increased by 11–13%; increased vascular permeability in response to ANP is abolished
GC-B dominant negative overexpression in rat [67]	Dominant-negative mutant for GC-B was fused with the CMV promoter	Whole body	No significant differences in systolic, diastolic and mean arterial pressure	Progressive cardiac hypertrophy, which was further enhanced in chronic volume overload	Reduced bone growth; modestly increased heart rate

Table 1. (Continued).

Mutated gene	Targeting construct	Targeted tissue	Blood pressure phenotype	Cardiac phenotype	Other phenotypes
GC-B dominant negative overexpression in mouse [60]	Dominant-negative mutant for GC-B, fused with promoter/enhancer regions of murine pro-α 1(II) collagen gene (Col2a1)	Cartilage	Not reported	Not reported	Significantly shorter nasoanal length
GC-B knockout [60]	Exons 3–7, encoding the C-terminal half of the extracellular ligand-binding domain and the transmembrane segment, were replaced by the neomycin resistance gene	Systemic disruption	No significant differences in blood pressure	Not reported	Impaired endochondral ossification, longitudinal vertebra or limb-bone growth; female infertility; impaired female reproductive tract development
C receptor knockout [28]	Most of exon 1 was replaced by the neomycin resistance gene	Systemic disruption	8 mmHg below normal	Not reported	Longer half-life of circulating ANP; reduced ability to concentrate urine; skeletal deformities with increased bone turnover

a standard-salt (0.5% NaCl) diet, the heterozygotes had normal circulating ANP levels and blood pressures. However, on high-salt (8% NaCl) diets, they were hypertensive, with 27 mmHg increases in systolic blood pressure levels [24].

In the same year, disruption of the *GC-A* gene was reported to result in chronically elevated blood pressure (about 25 mmHg in systolic pressure) in mice on a standard-salt diet [25]. Unlike mice heterozygous for the *ANP* gene, blood pressures of GC-A heterozygotes remained elevated and unchanged despite increasing dietary salt intake. In 1997, another group reported that the mice lacking functional *Npr1* gene, which encodes GC-A (denominated NPRA by the authors), displayed elevated blood pressure and cardiac hypertrophy with interstitial fibrosis resembling that seen in human hypertensive heart disease [26]. In a subsequent paper, the blood pressures of one-copy F1 animals were reported to be significantly higher on high-salt diet than on low-salt diet [27]. The reason for the discrepancy between the salt phenotypes of these two *GC-A* knockout mouse strains is still unknown. It is possible that differences result from different targeting strategies or the genetic background of the mouse strains used.

In 1999, the generation of mice in which the C receptor was inactivated by homologous recombination was reported [28]. C-receptor-deficient mice have less ability to concentrate urine, exhibit mild diuresis and tend to have depleted blood volume. C receptor homozygous mutants have significantly lower blood pressures (by 8 mmHg) than their wild-type counterparts. The half-life of ANP in C-receptor-deficient mice is two-thirds longer than that in wild-type mice, demonstrating that C receptor plays a significant role in its clearance. Moreover, C receptor modulates the availability of the natriuretic peptides to their target organs, thereby allowing the activity of the natriuretic peptide system to be tailored to specific local needs. In fact, C receptor expression is tightly regulated by other signaling molecules, such as angiotensin II [29] and catecholamines [30]. Interestingly, the baseline levels of ANP and BNP were not higher in the C-receptor-deficient mice than in the wild-type mice, implying that either the cardiac secretion or C-receptor-independent clearance mechanism was altered in those mice.

In 2000, the targeted disruption of the *BNP* gene in mice was reported. Multifocal fibrotic lesions were found in the ventricles of BNP-deficient mice, suggesting the protective role of BNP in pathological cardiac fibrosis [31]. Interestingly, there were no signs of systemic hypertension or ventricular hypertrophy, suggesting that in the presence of ANP basal levels of BNP are dispensable for these cardiovascular phenotypes.

To examine the tissue(s) responsible for the hypertensive phenotype of systemic GC-A-null mice, a targeting strategy was designed so that Cre recombinase mediates the deletion of exon 1 of the *GC-A* gene. Thus, in floxed GC-A mice, GC-A can be deleted in a tissue-specific manner. Endothelium-specific deletion of GC-A was achieved by crossing the floxed GC-A mice with transgenic mice expressing Cre recombinase under the control of the Tie2 promoter/enhancer. Endothelium-specific GC-A-deficient mice display significantly increased systolic blood pressure (by approximately 12–15 mmHg) and diastolic blood pressure (by approximately 5–10 mmHg) than their control littermates [32]. Interestingly, although the direct vasodilatation effects of exogenously administered ANP were abolished, smooth-muscle-cell-restricted deletion of GC-A did not affect the resting blood pressure [33], indicating that endothelial cell GC-A, and not vascular smooth muscle cell GC-A, is indispensable for chronic regulation of blood pressure.

Overall, these results show the significance of the endogenous natriuretic peptide system in the maintenance of normal blood pressure.

Regulation of blood volume

Infusion of ANP results in substantial natriuresis and diuresis in wild-type mice but fails to cause significant changes in sodium excretion or urine output in GC-A-deficient mice, indicating that GC-A is essential for ANP-induced acute regulation of diuresis and natriuresis [34]. After experimental expansion of the plasma volume, urine output as well as urinary sodium and cGMP excretion increase rapidly and markedly in the wild-type but not in systemic GC-A-deficient animals. Nevertheless, plasma ANP levels are comparable or even higher in CG-C-deficient animals [34]. On the contrary, the knock-in overexpression of GC-A (four-copy) in mice results in augmented responses to volume expansion in urinary flow and sodium excretion along with rises in both glomerular filtration rate and renal plasma flow, compared with wild-type (two-copy) mice after volume expansion [35]. These results establish that GC-A activation is the predominant mechanism mediating the natriuretic, diuretic and renal hemodynamic responses to acute blood volume expansion.

The plasma volumes of animals completely lacking GC-A are expanded by 30%, suggesting the role of GC-A in chronic regulation of the blood volume. Interestingly, mice lacking GC-A specifically in the vascular endothelium are volume expanded by 11–13% [32], suggesting that GC-A in the endothelium at least partly accounts for chronic blood volume regulatory effects. Since previous experiments indicated that ANP increased capillary permeability of the endothelium to macromolecules like albumin [36], these data suggest that the ANP/GC-A pathway regulates chronic transvascular fluid balance by increasing microvascular permeability [37].

Cardiac remodeling and the local natriuretic peptide system

Cardiac synthesis and secretion of ANP and BNP are increased according to the severity of cardiac remodeling in humans as well as in animal models [38]. Since the two cardiac natriuretic peptides share a common receptor (i.e. GC-A), the cardiac phenotype of mice lacking GC-A revealed complete effects of the cardiac natriuretic peptide signaling. Notably, targeted deletion of the *GC-A* gene resulted in marked cardiac hypertrophy and fibrosis, which were disproportionately severe [39,40] given the modest rise in blood pressure [25]. Since the chronic treatment of GC-A-deficient mice with anti-hypertensive drugs, which reduce blood pressure to levels similar to those seen in wild-type mice, has no significant effect on cardiac hypertrophy [41], these results imply that the natriuretic peptides/GC-A system has direct anti-hypertrophic effects in the heart, which are independent of its roles in blood pressure and body fluid control.

More direct evidence of local anti-hypertrophic GC-A signaling was obtained from animals in which the *GC-A* gene was conditionally targeted. The *GC-A* gene was selectively overexpressed in the cardiomyocytes of wild-type or *GC-A*-null animals, and the effects were examined [39]. Whereas introduction of the *GC-A* transgene did not alter blood pressure or heart rate as a function of genotype, it did reduce cardiomyocyte size in both wild-type and null backgrounds. The reduction in myocyte size was accompanied by a decrease in cardiac ANP mRNA expression, which suggests the existence of a local regulatory mechanism that governs cardiomyocyte size and gene expression via a GC-A-mediated pathway [42]. Conversely, the *GC-A* gene was inactivated selectively in cardiomyocytes by homologous loxP/Cre-mediated recombination, which circumvents the systemic hypertensive phenotype associated with germline disruption of the *GC-A* gene [43]. Mice with cardiomyocyte-restricted GC-A deletion exhibited mild cardiac hypertrophy with markedly increased transcription of cardiac hypertrophy markers, including ANP. These observations are consistent with the idea that a local function of the ANP/GC-A system is to moderate the molecular program of cardiac hypertrophy [44].